

We are IntechOpen, the world's leading publisher of Open Access books Built by scientists, for scientists

6,000

Open access books available

148,000

International authors and editors

185M

Downloads

Our authors are among the

154

Countries delivered to

TOP 1%

most cited scientists

12.2%

Contributors from top 500 universities



WEB OF SCIENCE™

Selection of our books indexed in the Book Citation Index
in Web of Science™ Core Collection (BKCI)

Interested in publishing with us?
Contact book.department@intechopen.com

Numbers displayed above are based on latest data collected.
For more information visit www.intechopen.com



Chapter

Charged Particle Beam Injection into Magnetically Confined Plasmas

Wonyong Chung, Andi Tan and Christopher Tully

Abstract

As the principles underpinning magnetic confinement are contrary to allowing significant heat flow via charged particles into or out of a magnetically confined plasma, the approach of charged particle beam injection has been largely overlooked. The method of magnetic orbital angular momentum beam acceleration, developed by the PTOLEMY experiment, provides a new avenue for injecting charged particle beams into high magnetic field regions. Initial simulations show how this novel acceleration method can yield charge, mass, and heat flow into toroidal magnetic fields with important implications for fusion energy science. This chapter will review this new method in the context of charged particle beam injection methods and the relevance of these tools for plasma and fusion science.

Keywords: charged particle beam injection, heating, magnetic confinement, magnetic gradient drift, ITER

1. Introduction

The dream of harnessing energy from controlled nuclear fusion has been proposed for several decades. Intensifying climate change issues increase the desire for a clean and safe energy source. A fusion reactor based on magnetic confinement provides a promising configuration for controlled thermonuclear fusion. To fuse nuclei with large densities for an extended period, it is necessary to heat the plasma to overcome the Coulomb repulsion. The power ratio, Q , of the fusion output power to the input power is proportional to the fusion product $nT\tau_E$, where n and T are the central ion density and temperature [1]. The parameter τ_E is the energy confinement time. In December 2021, the Joint European Torus (JET) achieved a new record and produced 59 MJ of energy with a Q of 0.33 over a τ_E of 5 s [2]. Although remarkable progress has been made to achieve the required n , T , and τ_E , they have not been achieved in the same reactor configuration simultaneously.

To achieve an ignition condition where self-sustaining fusion is possible, additional energy-efficient heating is required. Ohmic heating from the toroidal current wanes at high temperatures. Two external sources are typically used to provide heating power, the resonant absorption of radio frequency electromagnetic waves and the injection of energetic neutral particle beams.

The injected beams are neutralized to prevent reflection due to the magnetic field. The neutralization process introduces inefficiency and complicates the instrumentation.

Alternatives to neutral particle beam injection, typically for non-equilibrium fusion reactors, have been explored using different acceleration technologies [3, 4]. The challenges of energy efficiency in particle acceleration are formidable given the high fraction of input power needed to operate relatively low- Q fusion reactors. Radio-frequency acceleration cavities and time-varying electromagnetic fields are, in general, prone to internal ohmic losses and self-heating. Static accelerating fields avoid the bulk of these losses, but are suited primarily for charged particle beams. By construction, the insertion and extraction of charged particles from magnetic confinement systems is thwarted except when necessary, as in the case of divertors. However, non-confining trajectories can be constructed under special conditions through the same processes of cyclotron orbit drift that plague steady-state operation.

In the transverse drift electromagnetic filter developed for the PTOLEMY experiment (Princeton Tritium Observatory for Light, Early-Universe, Massive-Neutrino Yield), a compact configuration of electromagnetic fields simultaneously transports and decelerates energetic electrons from the tritium β -decay endpoint starting in high magnetic fields of several Tesla to regions where both the kinetic energy and magnetic fields are reduced by several orders of magnitude [5, 6]. A new method is devised to accelerate low-energy charged particles into a high magnetic field region by operating the PTOLEMY filter in “reverse.” This chapter presents the principles of this acceleration method and describes a possible application using the diagnostic port of the International Thermonuclear Experimental Reactor (ITER) [7].

2. Basics of charged particle beam injection

In this chapter, we use the convention that non-bolded symbols of vector quantities refer to the total magnitude unless a component is specified. The equation of motion of a charged particle of mass m and charge q in a magnetic field \mathbf{B} is given by

$$\frac{d}{dt} \left(m \frac{d\mathbf{r}}{dt} \right) = q \frac{d\mathbf{r}}{dt} \times \mathbf{B}. \quad (1)$$

The Lorentz force on the right-hand side is perpendicular to the particle’s velocity. In a uniform magnetic field, the particle’s motion projected on a plane perpendicular to the magnetic field is circular, with a gyroradius given by

$$\rho = \frac{mv_{\perp}}{qB} = \frac{\sqrt{2mT_{\perp}}}{qB}, \quad (2)$$

with T_{\perp} the transverse kinetic energy.

For a 1 MeV deuterium ion in a 5 T magnetic field, the gyroradius is about 0.04 m, a small fraction of a typical reactor radius. The ion beam injection energies must be relativistic to be commensurate with the reactor radius.

Relativistic ion beam injection introduces a number of inefficiencies. The plasma does not have the density required to stop energetic ions in a single transit, delivering limited power to the plasma and creating destructive irradiation of the reactor walls. The acceleration methods for relativistic beams involve time-varying fields that have several sources of intrinsic power loss.

In the following sections, charged particle injection of non-relativistic ions is re-examined as a transport mechanism that drifts charged ions from outside of the reactor volume to the surface of the plasma.

3. Magnetic orbital angular momentum beam acceleration

An alternative method to inject a charged particle beam is to create a beam of particles whose gyroradius is small compared to the transverse dimensions of the injection aperture. The particles are in cyclotron motion in a magnetic field that is relatively strong compared to their momentum. The acceleration mechanism stems from the ability of particles traveling in cyclotron motion in magnetic field gradients to do work. One, therefore, configures a magnetic geometry such that there is a transverse gradient along the average path of the beam. A complementary electric field is used to balance the gradient- B drift transverse to the average path of the beam and to accelerate the particles under the work of the magnetic field gradient. The acceleration process will be shown to be adiabatic for relevant injection energies and to maintain the magnetic moment invariance to a good accuracy after an initial stage of zero field ion source injection. The acceleration process does not affect the average linear momentum component of the beam. The increase in the charged particle kinetic energy follows from an increase in the magnetic orbital angular momentum.

3.1 Guiding-center drifts in adiabatic field conditions

When a charged particle gyrates in a magnetic field with a transverse gradient, the cyclotron-orbit averaged Guiding Center System (GCS) [8] motion can be described in terms of the drift terms of the virtual guiding-center particle if the spatial and temporal field variations within a single cyclotron orbit are taken to be adiabatic, i.e.,

$$\rho_c \ll \left| \frac{B}{\nabla B} \right|, \left| \frac{E}{\nabla E} \right|; \text{ and} \quad (3)$$

$$\tau_c \ll \left| \frac{B}{dB/dt} \right|, \left| \frac{E}{dE/dt} \right|; \quad (4)$$

where ρ_c is the Larmor radius and τ_c the cyclotron period. Under the conditions specified by Eq. (3) and (4), the first adiabatic invariant μ ,

$$\mu = \frac{mv_{\perp}^2}{2B} = \frac{T_{\perp}}{B}, \quad (5)$$

accurately describes an invariant quantity preserved in the motion of the particle [9, 10] and shows that an increase in the magnetic field magnitude is accompanied by a proportional increase in the transverse kinetic energy. Additionally, the deviation of the GCS trajectory from the direction of the magnetic field lines can be described in terms of four fundamental drift terms,

$$\mathbf{V}_D = \mathbf{V}_{\perp} = \left(q\mathbf{E} + \mathbf{F} - \mu\nabla B - m \frac{d\mathbf{V}}{dt} \right) \times \frac{\mathbf{B}}{qB^2}, \quad (6)$$

where V_{\perp} is the perpendicular component of the GCS velocity with respect to the magnetic field line. The transverse drift velocity, V_D , is composed of individual terms, as appear in Eq. (6) from left to right, known as (1) the $E \times B$ drift; (2) the external force drift; (3) the gradient- B drift; and (4) the inertial drift [8]. It is possible to configure the electric and magnetic field parameters to manipulate certain drift terms to produce a net linear trajectory in the transverse direction [5].

3.2 Drifts and work

The gradient- B drift is able to drive a charged particle up or down an electrostatic potential. This ability to do work, at first, seems contrary to the notion that magnetic fields do not do work on charged particles, as seen in Eq. (1), from the cross-product. Similarly, under the motion of $E \times B$ drift alone, the cross-product bars work as the electrons will drift on surfaces of constant voltage. This can also be understood by considering that it is always possible to boost into a frame in which the $E \times B$ drift is zero.

In contrast, a gradient- B drift due to a spatially varying magnetic field implies a time-varying electric field that cannot be boosted to zero. By itself, i.e., with a magnetic field and no electric field, a gradient- B does no work because there is nothing to do work against. However, when accompanied by an external $E \times B$ drift, the external electric potential provides a surface against which the gradient- B drift can do work on. The internal rotational kinetic energy of gyromotion of the virtual guiding-center particle is reduced for a corresponding increase in voltage potential. This is described by inserting terms from Eq. (6),

$$\frac{dT_{\perp}}{dt} = -q\mathbf{E} \cdot \mathbf{V}_D = -q\mathbf{E} \cdot (q\mathbf{E} - \mu\nabla B) \times \frac{\mathbf{B}}{qB^2} = \frac{\mu}{B^2} \mathbf{E} \cdot (\nabla B \times \mathbf{B}), \quad (7)$$

where T_{\perp} is the internal kinetic energy of gyromotion in the GCS frame [8].

3.3 Balanced drift

To produce a filter or accelerator based on the drift terms in Eq. (6), the external force and inertial drift terms are first taken to be zero, leaving only the electric and gradient- B drifts to be configured such that the total net drift is along a straight line parallel to the direction of the magnetic field gradient. The gradient- B drift alone is orthogonal to the direction of the magnetic field gradient, so the first step is to create a component of the $E \times B$ drift that exactly counters the gradient- B drift. From Eq. (6), this specifies the requirement,

$$q\mathbf{E}_{\parallel} \times \mathbf{B} = \mu\nabla B \times \mathbf{B}, \quad (8)$$

where E_{\parallel} is the component of electric field parallel to the magnetic field gradient. In general, the ratio of the parallel electric field to the magnitude of the magnetic field to meet this condition depends on the ratio μ/q times the fractional rate of change of the transverse component of the magnetic field along the direction of the magnetic field gradient. For an exponentially falling transverse field, the fractional rate of change is $1/\lambda$, the characteristic exponential length scale in units of transverse distance.

To introduce work, the electric field is tilted by adding an additional component, E_{\perp} , that is orthogonal to the direction of the magnetic field gradient. The $E_{\perp} \times B$ drift is what moves the charged particle either against or along the magnetic field gradient. As the components of E_{\parallel} and E_{\perp} are in vacuum, the relationship between the components follows from solving Maxwell's equations for a set of voltage plates above and below the direction of the balanced drift. Explicit solutions have been found [5]. Given that the magnitudes of E_{\parallel} and E_{\perp} are related, it is not surprising that the net drift velocity along the acceleration direction is constant. There is no linear momentum acceleration present. The acceleration occurs through the increase in the transverse kinetic energy component, the magnetic orbital angular momentum, during a process of constant drift along the magnetic field gradient.

3.4 Performance

Because the orbital magnetic moment $\mu = T_{\perp}/B$ is invariant, if the B field increases (or decreases) exponentially along the trajectory of the particle, so must its transverse kinetic energy. **Figure 1** shows the trajectory of a deuterium ion in a balanced drift with an initial kinetic energy of 20 keV at 0.2 T, going to a 4.7 T region with 1 MeV final kinetic energy. In this simulation, using CST studio [11], the magnetic field (**Figure 2**) is scaled from the one produced by the PTOLEMY magnet [6]. The maximum of the B_x field is set to 4.7 T at $Z = 1.6$ m to match the toroidal field near the interface of the upper port of ITER [12]. The electric field as in **Figure 3** is generated by a similar electrode structure as in the PTOLEMY transverse drift filter [6]. The dimensions are scaled up such that the distance between the electrodes is 0.3 m.

3.5 Injection

The net drift is along the direction of the magnetic field gradient and drives the guiding-center of the beam to cross equipotential lines and accelerates the particles. As the beam drifts in the direction of ∇B , it naturally reaches its maximum kinetic energy upon entering the toroidal magnet of a tokamak.

Via the foregoing mechanism, initial simulations of injecting deuterium ions indicate successful delivery of the beam, as shown in **Figure 4**. Once the particle leaves

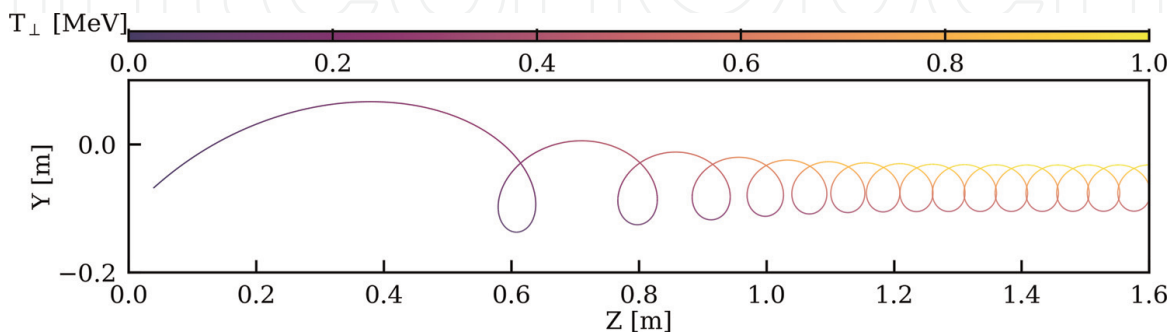


Figure 1. The trajectory of a deuterium ion in a transverse drift accelerator is shown with the low energy ion source on the left at a low magnetic field region and the high energy ion exiting the accelerator on the right in a region of high magnetic field. The net vertical drift is balanced to zero by construction as the ion drifts at constant velocity from left to right while climbing the magnetic field gradient. The trajectory is computed using the CST software suite. The color scale indicates the kinetic energy of the ion increasing from 20 keV at 0.2 T to 1 MeV at 4.7 T.

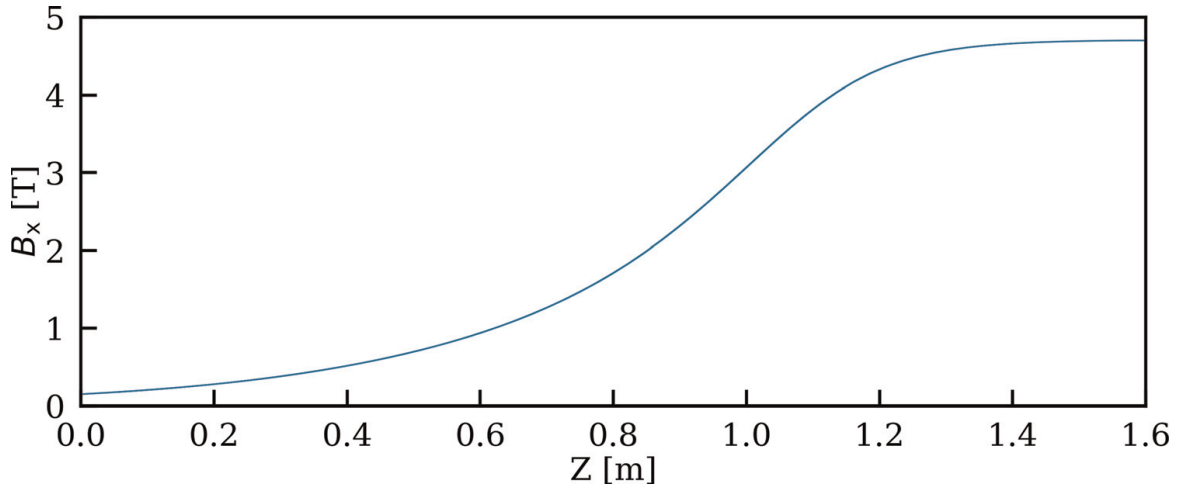


Figure 2. The profile of the transverse magnetic field in the CST simulation for the trajectory shown in **Figure 1**. It is derived from scaling the magnetic field produced by the PTOLEMY magnet to match a maximum B_x of 4.7 T.

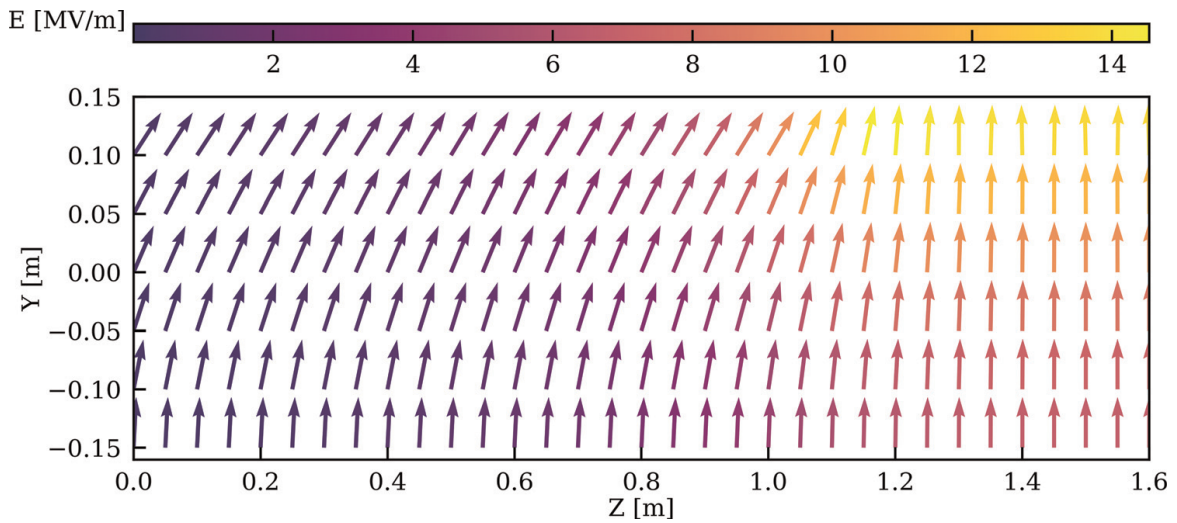


Figure 3. The electric field in the transverse plane in the drift region for the trajectory shown in **Figure 1**. The color (orientation) of the arrow indicates the magnitude (direction) of the field at its tail-end position.

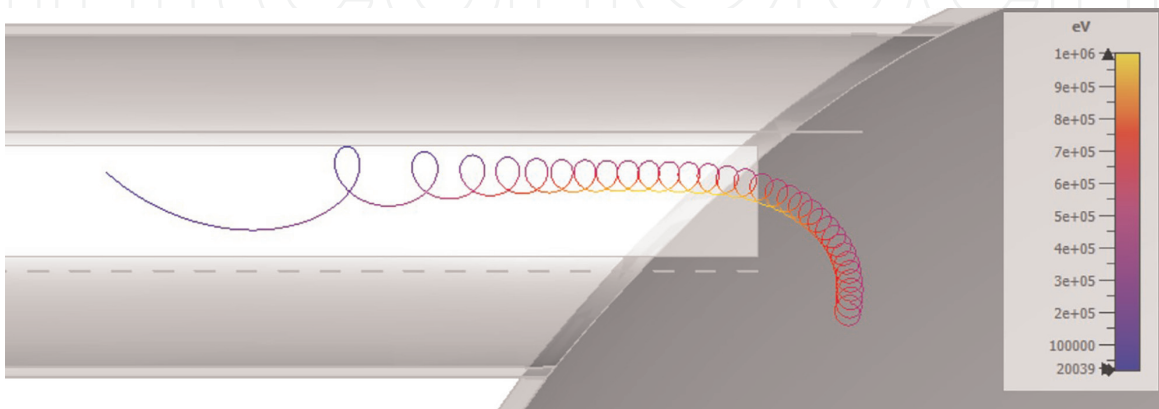


Figure 4. Simulation of the injection of deuterium ions into a $1/R$ magnetic field in a tokamak using the accelerating structure of **Figure 1**. Upon exiting the accelerator, the energetic ion continues to drift toward the plasma confinement region under the $1/R$ magnetic field gradient-B drift of the tokamak.

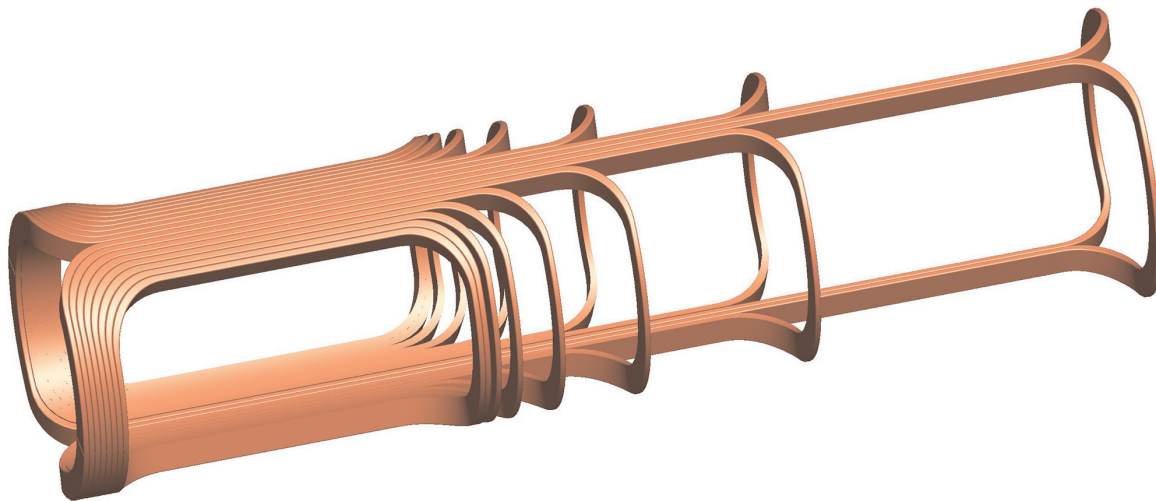


Figure 5.
A conceptual design of a tapered dipole magnet winding to generate the desired magnetic field for magnetic orbital angular momentum beam acceleration. The winding of the coils follows the surface of a cylindrical vacuum insertion port, similar to dipole magnets used in circular proton beam accelerators.

the injection port, the gradient of the $1/R$ toroidal magnetic field drifts the ions into the center of the plasma. The relatively hot thermal temperature of the 1 MeV deuterium ions will thermalize through Coulomb interactions with the plasma. The injection mechanism supports a range of injection energies and ion species. For instance, injection of 4 MeV α -particles through the ITER diagnostic port may be an effective way of studying the effects of fusion final-state ion interactions on the plasma. Charge neutralization can be achieved by instrumenting ion (electron) injection ports on the top (bottom) of the tokamak. The gradient- B drift will drift ions downward (for a given orientation of the azimuthal toroidal magnetic field) and electrons (or negative ions) upward.

The desired injection magnetic field, as described in Ref. [6], can be produced by a tapered dipole magnet with a superconductor winding, as in **Figure 5**.

A field cage with a number of electrodes can be placed inside the magnet to produce the corresponding electric field. Such a magnet is compact and can be placed within a counter-dipole coil in the upper diagnostic ports of ITER, as shown in **Figure 6**. The counter-dipole creates a zero field region for the ion source and reduces Lorentz forces on the primary reactor coils. The details of this magnet and the field cage are beyond the scope of this chapter.

4. Energy efficiency

An important aspect of magnetic orbital angular momentum acceleration for fusion energy efficiency is the reliance solely on static electric and magnetic fields. The power loading during injection on the accelerating plate voltages draws from highly efficient DC power supplies. Above all, the largest inefficiency of neutral beam injection, the neutralization, is avoided with direct charged particle injection. The high currents and efficient production of positive ions saves on power losses at the source relative to the negative ion beams used for neutral beam injection [13]. The inefficiencies and beam energy limitations associated with neutralization and

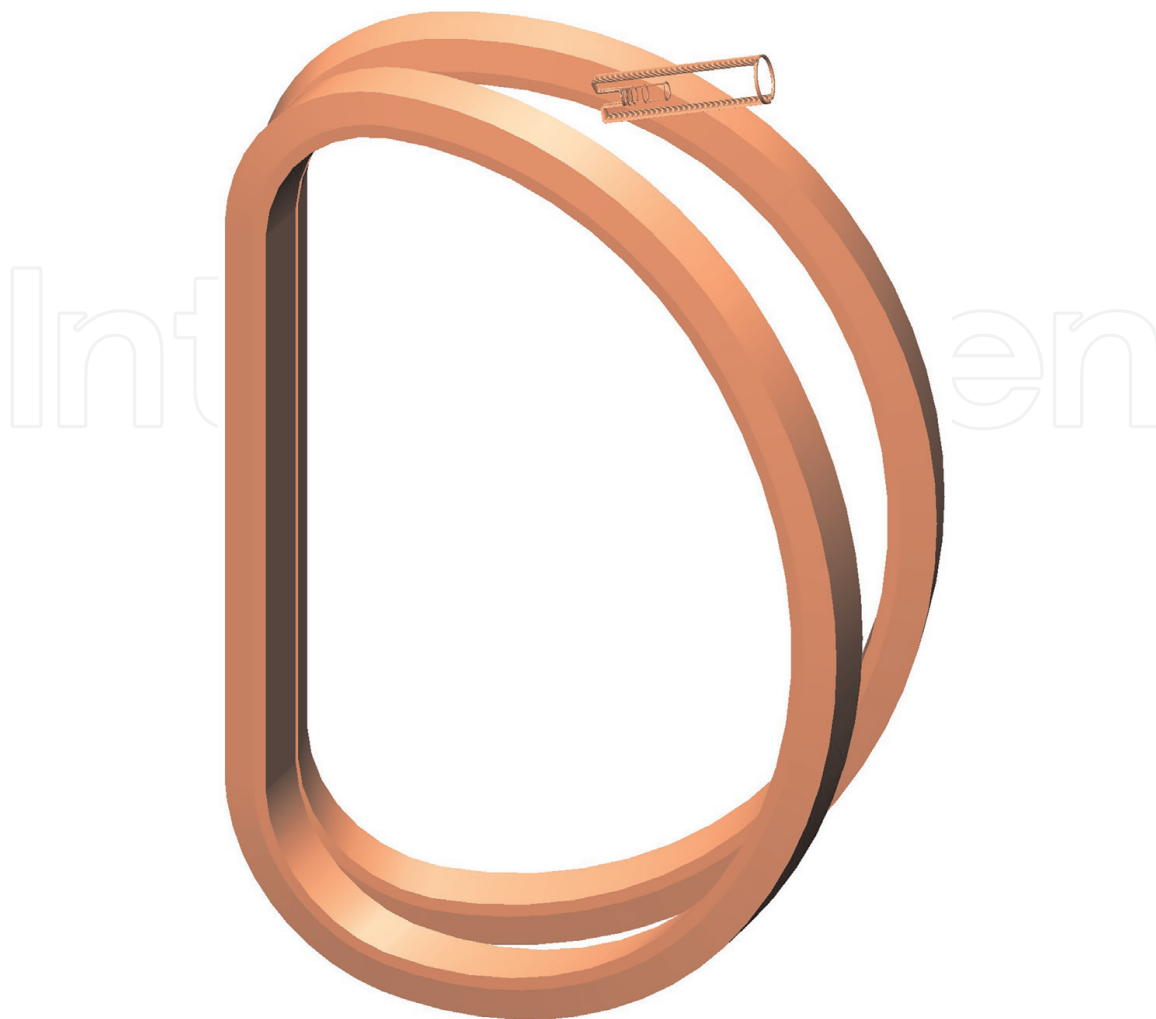


Figure 6. A tapered dipole magnet, as shown in **Figure 5**, with a counter-dipole winding placed in the upper port between two adjacent ITER toroidal field coils. The counter-dipole reduces the magnetic forces between the injection system and the tokamak field windings.

neutral beam injection introduce approximately a factor of 2 loss in absolute power efficiency [14].

5. Conclusions

Fusion reactor science is on the brink of a major advance toward sustained clean energy reactors. Reducing inefficiency in the particle beam injection systems is a promising direction toward achieving ignition conditions without compromising reactor operation. A surprising and yet potentially revolutionary approach to improving beam heating is through a new particle acceleration method called magnetic orbital angular momentum beam acceleration. With this technique, charged particle beam injection into magnetically confined plasmas becomes possible. The relevant parameters for charged particle beam injection are presented with simulated geometries demonstrating the feasibility of implementing this system with the diagnostic port of ITER. Charged particle beam injection provides a new tool for fusion reactors to deliver charge, mass, and heat flow into the plasma. The large gain in energy efficiency for charged particle injection is the most advantageous factor in comparing with neutral beam injection.

Acknowledgements

This research was supported by the Simons Foundation (#377485) and the John Templeton Foundation (#61814).

IntechOpen


IntechOpen

Author details

Wonyong Chung, Andi Tan* and Christopher Tully
Department of Physics, Princeton University, Princeton, New Jersey, USA

*Address all correspondence to: andit@princeton.edu

IntechOpen

© 2022 The Author(s). Licensee IntechOpen. This chapter is distributed under the terms of the Creative Commons Attribution License (<http://creativecommons.org/licenses/by/3.0>), which permits unrestricted use, distribution, and reproduction in any medium, provided the original work is properly cited. 

References

- [1] Wesson J, Campbell DJ. Tokamaks. Oxford, England: Oxford University Press; 2011. Available online: <https://global.oup.com/academic/product/tokamaks-9780199592234>
- [2] Gibney E. Nuclear-fusion reactor smashes energy record. *Nature*. 2022; **602**(7897):371-371
- [3] Liu KF, Chao AW. Accelerator based fusion reactor. *Nuclear Fusion*. 2017; **57**(8):084002
- [4] Labaune C, Baccou C, Depierreux S, Goyon C, Loisel G, Yahia V, et al. Fusion reactions initiated by laser-accelerated particle beams in a laser-produced plasma. *Nature Communications*. 2013; **4**(1):1-6
- [5] Betti MG, Biasotti M, Bosca A, Calle F, Carabe-Lopez J, Cavoto G, et al. A design for an electromagnetic filter for precision energy measurements at the tritium endpoint. *Progress in Particle and Nuclear Physics*. 2019; **106**:120-131
- [6] Apponi A, Betti MG, Borghesi M, Canci N, Cavoto G, Chang C, et al. Implementation and optimization of the PTOLEMY transverse drift electromagnetic filter. *Journal of Instrumentation*. 2022; **17**(05):P05021. DOI: 10.1088/1748-0221/17/05/p05021
- [7] International Thermonuclear Experimental Reactor (ITER). 2022. Available from: <http://www.iter.org> [Accessed: 2022-06]
- [8] Roederer J, Zhang H. Particle fluxes, distribution functions and violation of invariants. In: *Dynamics of Magnetically Trapped Particles*. Berlin, Heidelberg: Springer-Verlag; 2014. pp. 89-122. Available online: <https://link.springer.com/book/10.1007/978-3-642-41530-2>
- [9] Alfvén H. On the motion of a charged particle in a magnetic field. *Arkiv foer Matematik, Astronomi, och Fysik*. 1940; **25B**(1-20):29
- [10] Cary JR, Brizard AJ. Hamiltonian theory of guiding-center motion. *Reviews of Modern Physics*. 2009; **81**(2):693
- [11] Dassault Systèmes. CST Studio Suite; Available from: <http://www.cst.com>
- [12] International Atomic Energy Agency. Summary of the ITER Final Design Report. No. 22 in ITER EDA Documentation Series. Vienna: International Atomic Energy Agency; 2001. Available from: <https://www.iaea.org/publications/6442/summary-of-the-iter-final-design-report>
- [13] Hemsworth RS, Inoue T. Positive and negative ion sources for magnetic fusion. *IEEE Transactions on Plasma Science*. 2005; **33**(6):1799-1813
- [14] Hopf C, Starnella G, den Harder N, Fantz U. Neutral beam injection for fusion reactors: Technological constraints versus functional requirements. *Nuclear Fusion*. 2021; **61**(10):106032. DOI: 10.1088/1741-4326/ac227a